catalysts

MDPI

Article

CuO Nanorods-Decorated Reduced Graphene Oxide Nanocatalysts for Catalytic Oxidation of CO

Yan Wang [1], Zhihui Wen [1,*], Huoli Zhang [2], Guohua Cao [2], Qi Sun [2] and Jianliang Cao [2,*]

[1] School of Safety Science and Engineering, State Key Laboratory Cultivation Base for Gas Geology and Gas Control, Henan Polytechnic University, Jiaozuo 454000, China; yanwang@hpu.edu.cn

[2] School of Chemistry and Chemical Engineering, Henan Polytechnic University, Jiaozuo 454000, China; zhanghuoli@hpu.edu.cn (H.Z.); ghcao@hpu.edu.cn (G.C.); qisun_l@hotmail.com (Q.S.)

* Correspondence: wenzhihui@hpu.edu.cn (Z.W.); caojianliang@hpu.edu.cn (J.C.); Tel.: +86-391-398-7440 (Z.W. & J.C.)

Academic Editors: Shaobin Wang and Xiaoguang Duan
Received: 18 November 2016; Accepted: 13 December 2016; Published: 21 December 2016

Abstract: Developing an efficient non-noble catalyst for CO oxidation with high catalytic activity remains a challenge for practical applications. In this work, CuO nanorods decorated reduced graphene oxide (RGO) nanocatalysts were prepared via a facile one-step hydrothermal method. The structure and morphology of the as-prepared samples were characterized by XRD, Raman spectroscopy, SEM, TEM, and X-ray photoelectron spectroscopy (XPS). The analysis results show that CuO nanorods were successfully deposited on the surface of RGO sheets with the length of 250–500 nm. The catalytic properties of the as-prepared catalysts for CO oxidation were evaluated by using a microreactor-gas chromatograph (GC) system. The as-prepared RGO–CuO nanocatalysts exhibited high activity for CO oxidation, and the 10 wt % reduced graphene oxide content catalyst can achieve CO total oxidation at 165 °C.

Keywords: CuO nanorods; reduced graphene oxide; heterogeneous catalysis; CO; catalytic oxidation

1. Introduction

Carbon monoxide (CO) is an odorless and poisonous gas, and a small amount is fatal. Catalytic oxidation is a good removal method, even for low concentrations of CO. The catalytic oxidation of CO is one of the simplest and the most extensively investigated reactions in heterogeneous catalysis [1–10], and the catalytic oxidation of CO has become an important research topic over the past years. Up to now, many very effective noble metal catalysts, such as Pd [3,11], Au [4,12], Ru [13,14], and Pt [5,15] have been developed for this reaction. However, the poor stability and high cost limit the applications of these noble metal catalysts.

In recent years, much attention was given to seeking non-noble metal catalysts such as Cu [7,9,16], Mn [17], and Co [18–20] to reduce the price and realize high-efficiency CO conversion. In all of these base metal CO oxidation catalysts, supported copper catalysts on Fe_2O_3, CeO_2, ZrO_2, and Ce-Zr-O exhibited very high catalytic activities similar to noble metal catalysts. Our previous studies [2,7] also showed that copper oxide possesses almost the same catalytic activity to CO oxidation as the noble metal catalysts.

As is known, the nature of the support is of crucial importance to the good catalytic performance of the resultant catalysts. Many investigations have demonstrated that the high surface area of the supports would give rise to well-dispersed and stable CuO active species nanoparticles on the surface upon calcination and reduction, which would further lead to an improved catalytic performance [2,9]. At the same time, the supported catalysts can show a synergistic effect to induce properties that are different from those of each individual component.

Because of its unique structure, intrinsic properties, and easy surface modification [21], graphene has been regarded as one of the most excellent supports for various catalysts. Graphene-supported Pd [3], Pt [22], TiO_2 [23], CeO_2 [24], and MnO_2 [25] materials have been recently reported to possess high activities in many catalytic reactions. In the theoretical research field, some studies have predicted that graphene-based catalysts may possess high activity for CO oxidation [26,27]. However, to the best of our knowledge, there are still no reports of experimental work for the catalytic application of graphene–CuO hybrids for catalytic CO oxidation.

In this paper, we report a facile hydrothermal method for the preparation of a series of reduced graphene oxide (RGO)–CuO hybrid nanocatalysts with different RGO contents for CO oxidation. The interaction between CuO and reduced graphene oxide was further investigated. The as-prepared hybrid nanocatalysts were characterized by various material characterization techniques, including XRD, Raman spectroscopy, SEM, TEM, and X-ray photoelectron spectroscopy (XPS). Catalytic activity tests of the as-prepared RGO–CuO nanocatalysts for CO oxidation were performed on a continuous-flow fixed-bed microreactor-gas chromatograph system.

2. Results and Discussion

2.1. Catalyst Characterization

The X-ray diffraction patterns of pure CuO, RGO, and the as-prepared RGO–CuO hybrid nanocatalysts with different RGO contents are shown in Figure 1. It can be clearly seen from Figure 1 that the broad diffraction peak at 25.1° is attributed to the (002) plane of the hexagonal graphite structure [28], which illustrates that graphene was successfully prepared. Meanwhile, all the peaks of CuO composites clearly show the monoclinic system of CuO (JCPDS no. 05-0661) [29]. The sharp peaks of the composites indicate that CuO has a high degree of crystallinity. However, there is no obvious characteristic peaks of graphene in the composites, which may be due to the lesser content of graphene or the strong CuO peaks covering the graphene peaks.

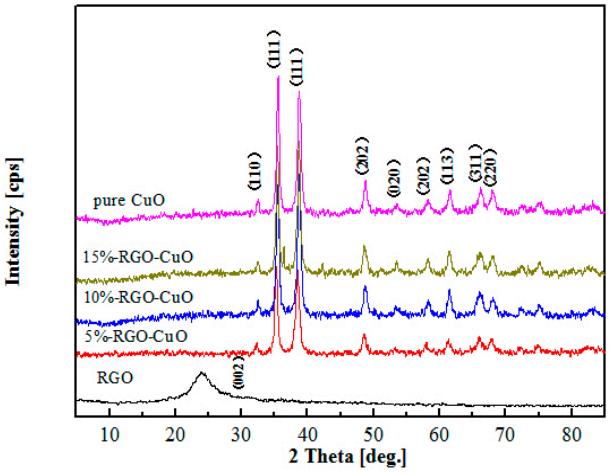

Figure 1. XRD patterns of the reduced graphene oxide (RGO), pure CuO, and RGO–CuO composites.

Raman spectroscopy is convenient, and one of the most important techniques for the characterization of graphitic materials. Figure 2 shows the Raman spectrum of the RGO–CuO hybrid nanocatalysts with different RGO contents. From Figure 2, one can see that the broad peaks displayed at 1350 and 1575 cm^{-1} are assigned to the D band (κ-point phonons of A_{1g} symmetry) and G band (E_{2g} phonon of C sp^2 atoms) [30], which confirm the presence of graphene in the hybrid composites. In addition, there are two typical peaks at around 343 and 640 cm^{-1} observed for the RGO–CuO hybrid nanocatalysts, which are characteristics of a CuO phase [22,31].

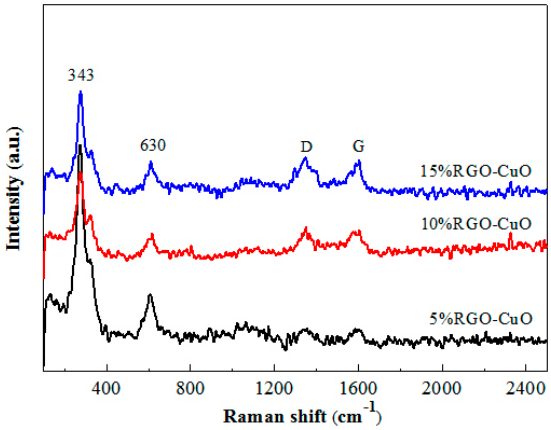

Figure 2. Raman spectra of RGO–CuO composites.

SEM images were taken for the 10%-RGO–CuO hybrid composite to investigate the morphology of the as-prepared samples, as shown in Figure 3. It can be clearly seen from Figure 3 that the RGO–CuO hybrid composite is constructed by CuO nanorods and RGO nanosheets, and that both of them are wrapped closely together. The RGO is decorated with rod-like CuO with typical diameters of 30–150 nm and lengths of 250–500 nm, and the CuO nanorods are distributed randomly.

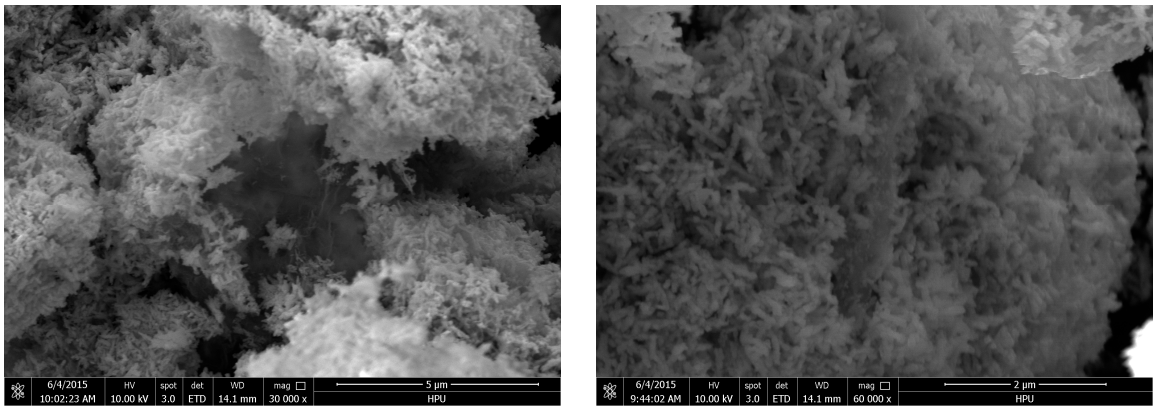

(**a**) (**b**)

Figure 3. SEM images of the 10%-RGO–CuO hybrid naocatalysts with (**a**) low magnification and (**b**) high magnification.

The structure of the as-prepared 10%-RGO–CuO hybrid composite was further observed by TEM analysis, as shown in Figure 4. One can see from Figure 4 that CuO nanorods were compactly anchored on the surface of RGO nanosheets. RGO nanosheets with clear wrinkles were obviously observed in the hybrid nanocomposite.

XPS analysis was performed to clarify the valence states of the elements present in the RGO–CuO hybrid composite nanocatalyst, and the results are shown in Figure 5. Figure 5a shows the general survey spectrum, which reveals that the surface of the RGO–CuO hybrid composite nanocatalyst contains C, O, and Cu elements. Figure 5b shows the Cu 2p spectra of the composite nanocatalyst, and the peaks located at 933.5 eV and 953.7 eV can be assigned to the binding energy of $Cu_{2p3/2}$ and $Cu_{2p1/2}$, respectively. The appearance of a shake-up peak at 940.6–944.5 eV demonstrated that the Cu species on the surface of the composite catalyst is Cu^{2+} [32]. Figure 5c shows the C 1s spectra of the composite catalysts, and the main peak at 284.6 eV was further separated into three peaks at 284.6, 286.6, and 288.9 eV, corresponding to the sp^2-hybridized carbon bonds, C–OH, and –O–C=O groups [33]. The peaks of oxygen-containing functional groups are much weaker than that of sp^2 C–C,

which demonstrated that GO transformed almost completely into graphene. Figure 5d exhibits two asymmetric peaks at 530.2 and 531.5 eV, which illustrated that two different oxygen species existed on the surface of the composite catalysts. The peak at 530.2 eV is assigned to lattice oxygen, and the other is the weakly adsorbed oxygen ion (O^-) on the surface of the hybrid composite nanocatalyst.

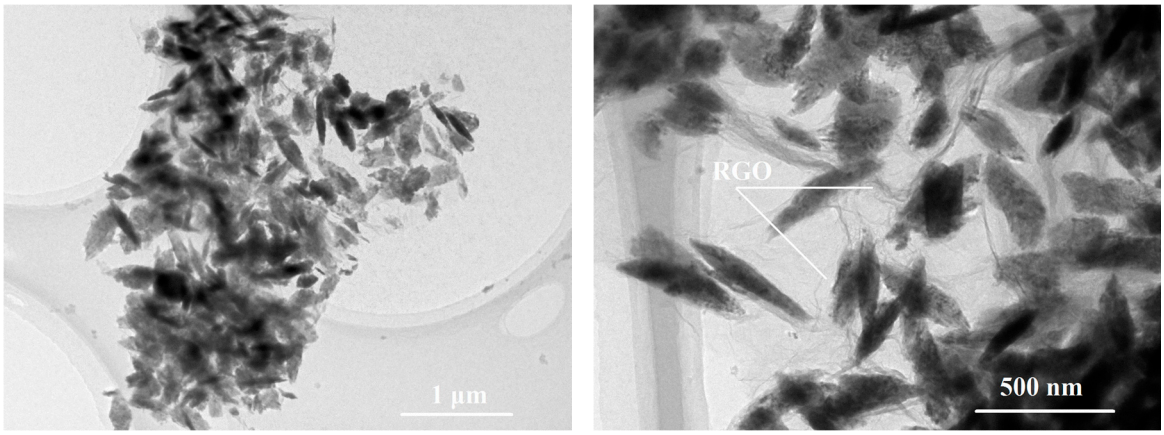

Figure 4. TEM images of the 10%-RGO–CuO hybrid naocatalysts with (**a**) low magnification and (**b**) high magnification.

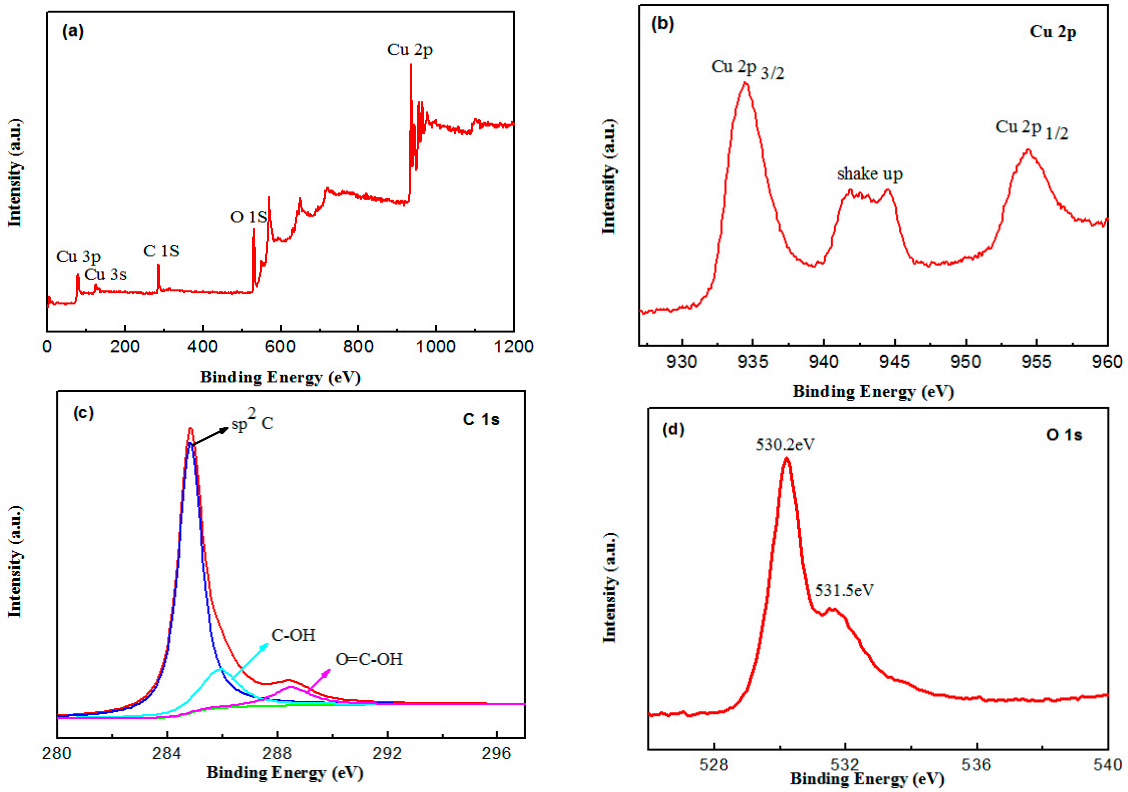

Figure 5. XPS analysis of the 10%-RGO–CuO catalyst: (**a**) general scan; (**b**) Cu 2p spectrum; (**c**) C 1s spectrum; (**d**) O 1s spectrum.

2.2. Catalytic Activity

Catalytic CO oxidation activities of the as-prepared RGO–CuO hybrid nanocatalysts were tested by using a microreactor-gas chromatograph (GC) system, as shown in Figure 6. Figure 6a exhibits

the catalytic activity for CO oxidation in the temperature range of 100–210 °C. Under the reaction conditions, all of the as-prepared catalysts presented with similar regularity that CO conversion increased with the increase of the reaction temperature. The pure graphene support had no activity, while all the hybrid nanocatalysts had much higher activities than the pure graphene support. In addition, all the RGO–CuO hybrid nanocatalysts possessed much higher CO oxidation activity than that of pure CuO, which could be ascribed to the addition of reduced graphene oxide, and there may have an interaction between CuO nanorods and the graphene support—this synergistic effect could strongly affect their catalytic CO oxidation activities. We can also see from Figure 6a that the activity of the RGO–CuO hybrid nanocatalysts enhanced with the increase of graphene content, and the 10%-RGO–CuO could achieve total CO oxidation at 165 °C. However, further increased graphene content resulted in a decrease in the catalytic CO oxidation activity.

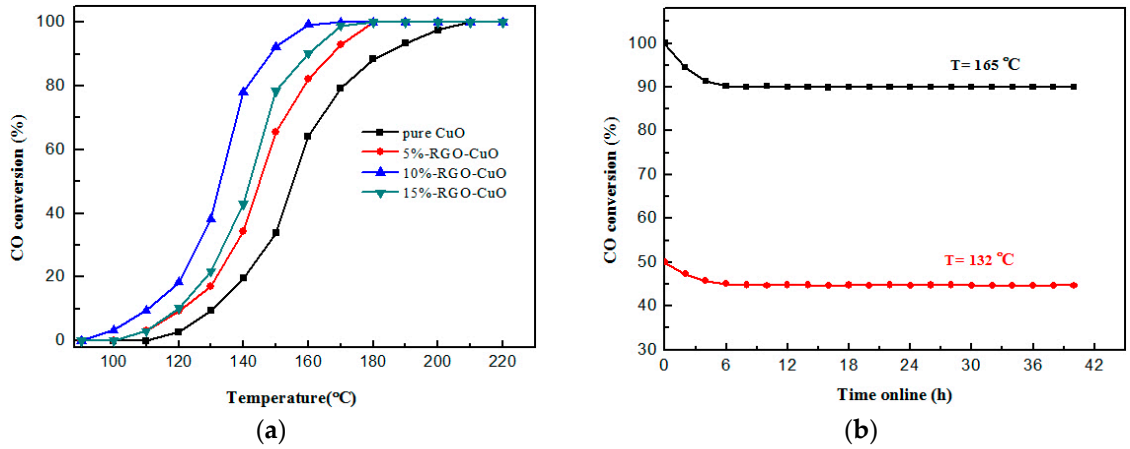

Figure 6. (**a**) Catalytic activity for CO oxidation of the pure CuO and RGO–CuO catalyst with different RGO contents; (**b**) CO conversion over the 10%-RGO–CuO catalyst at 132 °C and 165 °C as a function of reaction time.

The 10%-RGO–CuO catalyst was selected to investigate the catalytic stability for CO of the as-prepared RGO–CuO hybrid nanocatalysts. Figure 6b shows CO conversion over the 10%-RGO–CuO catalyst at 132 °C (T_{50}) and 165 °C (T_{100}) as a function of reaction time. It can be clearly seen that the CO conversion decreased slightly at the beginning of the 6 hours, and then the CO conversion remained basically unchanged. The decreasing activity may be ascribed to two factors: one is that the surface composition of the catalyst is not stable at the beginning time, and the other is that the interaction between the reactant and the catalyst surface has not yet reached the redox equilibrium. In a word, the results demonstrated that the catalytic activity of the as-prepared RGO–CuO composite catalysts was steady.

3. Materials and Methods

3.1. Synthesis

Graphene oxide (GO) was prepared by the method of Hummers [34] from natural graphite powder (≤30 μm) supplied by Sinopharm Chemical Regent Co., Ltd. (shanghai, china). The RGO–CuO composites were synthesized by a facile hydrothermal method. In a typical process, 2.375 g of $Cu(CH_3COO)_2$ was dissolved in 50 mL distilled water. The corresponding amount of GO solution (1.12 wt %) was added into 200 mL of distilled water under ultrasonication for 60 min. The above two solutions were mixed and then stirred for 20 min. Then, 50 mL of aqueous NaOH solution (0.5 mol/L) and 0.3 g of sodium borohydride ($NaBH_4$) were added into the above mixed solution in turn, and then stirred for another 30 min. Subsequently, the resulting solution was transferred into a 500 mL Teflon-lined stainless steel autoclave and heated to 180 °C for 24 h, and then cooled to room

temperature in an oven. Finally, the precipitate was collected by centrifuging. Then, the precipitate was washed with distilled water three times and ethanol two times, respectively. Following this, the precipitate was dried in air at 60 °C for 8 h. The obtained catalysts were marked as *x*-RGO–CuO (x = GO/(GO + CuO) = 5%, 10%, 15%). For comparison, pure CuO and RGO were also prepared by the same method. A flow chart of the preparation process is presented in Figure 7.

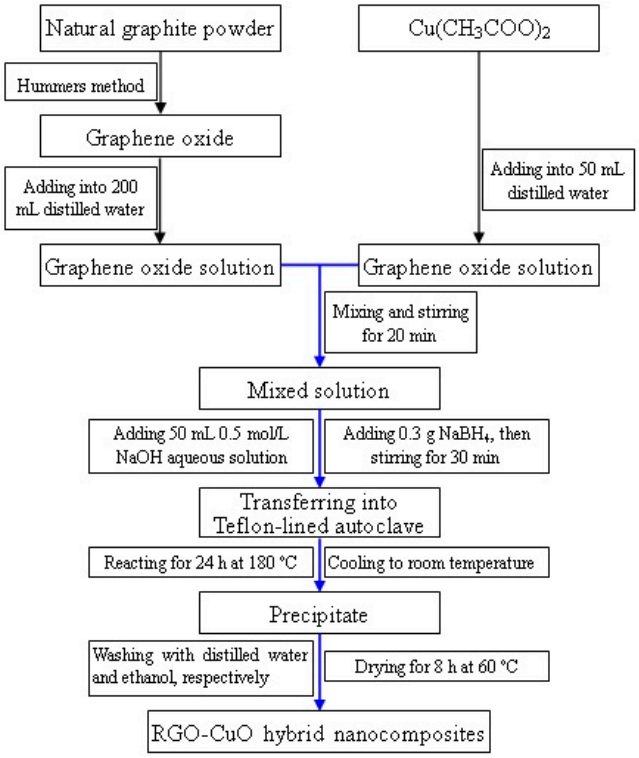

Figure 7. Preparation process of RGO–CuO hybrid nanocomposites.

3.2. Characterizations

The as-prepared nanocatalysts were characterized by X-ray diffraction (XRD, Bruker-AXS D8, Bruker, Madison, WI, USA) with CuKα radiation at 40 kV and 25 mA. Raman spectra were recorded by using a Renishaw inVia Reflex Raman Microscope (Renishaw plc, Wotton-under-Edge, Glos., UK). X-ray photoelectron spectroscopy (XPS) measurements were measured on a Perkin-Elmer PHI 5600 spectrophotometer (Perkin Elmer Limited, Waltham Mass, Waltham, MA, USA)with MgK_{α} (1253.6 eV) radiation. The structure and morphology of the samples were observed by field-emission scanning electron microscopy (FESEM, Quanta™250 FEG) (FEI, Eindhoven, The Netherlands). Transmission electron microscopy (TEM) analysis was performed on a JEOL JEM-2100 microscope (JEOL, Tokyo, Japan) operating at 200 kV.

3.3. Catalytic Performance

Catalytic activity tests for low-temperature CO oxidation were carried out on a fixed-bed continuous-flow 8 mm inner diameter steel tube reactor under ambient pressure. About 400 mg of catalyst powder was placed into the reactor. The mixed gas of 10 vol % CO balanced with air passed through the steel reactor with a flow rate of 73.2 mL/min. After 30 min of reaction, we analyzed the effluent gases online by a GC-6890 gas chromatograph (Tengzhou, Shandong, China). The catalytic activity was expressed by the conversion of CO.

$$\text{Conversion of CO} = \frac{[CO_2]_{out}}{[CO]_{out} + [CO_2]_{out}} \times 100$$

4. Conclusions

In summary, the CuO nanorods decorated reduced graphene oxide RGO–CuO hybrid nanocatalysts were successfully synthesized by a facile hydrothermal method. The RGO–CuO composite nanocatalysts exhibit high catalytic activity and stability for CO oxidation. The enhanced catalytic property can be attributed to the addition of graphene and the interaction between CuO and reduced graphene oxide. In addition, the nanorod structure of CuO can provide more active sites for CO oxidation. The 10%-RGO–CuO catalyst exhibits the highest catalytic activity for CO total oxidation at 165 °C. This facile synthesis method is promising for the preparation of other graphene-based composite materials for CO oxidation reaction.

Acknowledgments: This work was supported by the National Natural Science Foundation of China (51504083, 51404097, 51301062), China Postdoctoral Science Foundation funded project (2016M592290), Program for Science & Technology Innovation Talents in Universities of Henan Province (17HASTIT029), Program for Innovative Research Team (in Science and Technology) in the University of Henan Province (16IRTSTHN005), the Fundamental Research Funds for the Universities of Henan Province (NSFRF140101) and Foundation for Distinguished Young Scientists of Henan Polytechnic University (J2016-2, J2017-1).

Author Contributions: Yan Wang conceived and designed the experiments; Huoli Zhang, Qi Sun and Guohua Cao performed the experiments and analyzed the data; Zhihui Wen and Jianliang Cao provided the concept of this research and managed all the experimental and writing process as the corresponding authors.

Conflicts of Interest: The authors declare no conflict of interest.

References

1. Aguila, G.; Guerrero, S.; Araya, P. Effect of the preparation method and calcination temperature on the oxidation activity of CO at low temperature on CuO-CeO_2/SiO_2 catalysts. *Appl. Catal. A Gen.* **2013**, *462–463*, 56–63. [CrossRef]
2. Cao, J.; Wang, Y.; Zhang, Y.; Wu, S.; Yuan, Z. Preparation, characterization and catalytic behavior of nanostructured mesoporous CuO/$Ce_{0.8}Zr_{0.2}O_2$ catalysts for low-temperature CO oxidation. *Appl. Catal. B Environ.* **2008**, *78*, 120–128. [CrossRef]
3. Li, Y.; Yu, Y.; Wang, J.; Song, J.; Li, Q.; Dong, M.; Liu, C. CO oxidation over graphene supported palladium catalyst. *Appl. Catal. B: Environ.* **2012**, *125*, 189–196. [CrossRef]
4. Haruta, M.; Tsubota, S.; Kobayashi, T.; Kageyama, H.; Cenet, M.; Delmon, B. Low-temperature oxidation of CO over gold supported on TiO_2, α-Fe_2O_3, and Co_3O_4. *J. Catal.* **1993**, *144*, 175–192. [CrossRef]
5. Engel, T.; Ertl, G. Elementary steps in the catalytic oxidation of carbon monoxide on platinum metals. *Adv. Catal.* **1979**, *28*, 1–78.
6. Zhu, D.; Duan, D.; Han, Y.; He, Y.; Chen, Y.; Zhang, W.; Yan, Z.; Wang, J.; Yuan, F. Noble Metal-Free Ceria-Zirconia Solid Solutions Templated by Tabacco Materials for Catalytic Oxidation of CO. *Catalysis* **2016**, *6*, 135.
7. Cao, J.; Wang, Y.; Yu, X.; Wang, S.; Wu, S.; Yuan, Z. Mesoporous CuO–Fe_2O_3 composite catalysts for low-temperature carbon monoxide oxidation. *Appl. Catal. B Environ.* **2008**, *79*, 26–34. [CrossRef]
8. Yang, W.; Zhang, R.; Chen, B.; Bion, N.; Duprez, D.; Royer, S. Activity of perovskite-type mixed oxides for the low-temperature CO oxidation: Evidence of oxygen species participation from the solid. *J. Catal.* **2012**, *295*, 45–48. [CrossRef]
9. Luo, M.; Ma, J.; Lu, J.; Song, Y.; Wang, Y. High-surface area CuO–CeO_2 catalysts prepared by a surfactant-templated method for low-temperature CO oxidation. *J. Catal.* **2007**, *246*, 52–59. [CrossRef]
10. Lin, H.; Chiu, H.; Tsai, H.; Chien, S.; Wang, C. Synthesis, characterization and catalytic oxidation of carbon monoxide over cobalt oxide. *Catal. Lett.* **2003**, *88*, 169–174. [CrossRef]
11. Chen, S.; Si, R.; Taylor, E. Synthesis of Pd/Fe_3O_4 hybrid nanocatalysts with controllable interface and enhanced catalytic activities for CO oxidation. *J. Phys. Chem. C* **2012**, *116*, 12969–12976. [CrossRef]
12. Avgouropoulos, G.; Manzoli, M.; Boccuzzi, F.; Tabakova, T.; Papavasiliou, J.; Idakiev, V. Catalytic performance and characterization of Au/doped-ceria catalysts for the preferential CO oxidation reaction. *J. Catal.* **2008**, *256*, 237–247. [CrossRef]
13. Kim, Y.; Park, E. The effect of the crystalline phase of alumina on the selective CO oxidation in a hydrogen-rich stream over Ru/Al_2O_3. *Appl. Catal. B Environ.* **2010**, *96*, 41–50. [CrossRef]

14. Chen, H. First-principles study of CO adsorption and oxidation on Ru-doped CeO_2 (111) surface. *J. Phys. Chem. C* **2012**, *116*, 6239–6246. [CrossRef]
15. Chua, Y.P.G.; Gunasooriya, G.T.K.K.; Saeys, M.; Seebauer, E.G. Controlling the CO oxidation rate over Pt/TiO_2 catalysts by defect engineering of the TiO_2 support. *J. Catal.* **2014**, *311*, 306–313. [CrossRef]
16. Svintsitskiy, D.A.; Kardash, T.Y.; Stonkus, O.A. In situ XRD, XPS, TEM, and TPR study of highly active in CO oxidation CuO nanopowders. *J. Phys. Chem. C* **2013**, *117*, 14588–14599. [CrossRef]
17. Xiao, J.; Wan, L.; Wang, X.; Kuang, Q.; Dong, S.; Xiao, F.; Wang, S. Mesoporous Mn_3O_4–CoO core–shell spheres wrapped by carbon nanotubes: A high performance catalyst for the oxygen reduction reaction and CO oxidation. *J. Mater. Chem. A* **2014**, *2*, 3794–3800. [CrossRef]
18. Hu, L.; Sun, K.; Peng, Q.; Xu, B.; Li, Y. Surface active sites on Co_3O_4 nanobelt and nanocube model catalysts for CO oxidation. *Nano Res.* **2010**, *3*, 363–368. [CrossRef]
19. Radwan, N.R.E.; El-Shall, M.S.; Hassan, H.M.A. Synthesis and characterization of nanoparticle Co_3O_4, CuO and NiO catalysts prepared by physical and chemical methods to minimize air pollution. *Appl. Catal. A Gen.* **2007**, *331*, 8–18. [CrossRef]
20. Jia, M.; Zhang, W.; Tao, Y.; Wang, G.; Cui, X.; Zhang, C.; Wu, T.; Dong, G. Preparation, characterization and CO oxidation of nanometer Co_3O_4. *Chem. Res. Chin. Univ.* **1999**, *4*, 637–639.
21. Machado, B.F.; Serp, P. Graphene-based materials for catalysis. *Catal. Sci. Technol.* **2012**, *2*, 54–75. [CrossRef]
22. Yoo, E.; Okata, T.; Akita, T.; Kohyama, M.; Nakamura, J.; Honma, I. Enhanced electrocatalytic activity of Pt subnanoclusters on graphene nanosheet surface. *Nano Lett.* **2009**, *9*, 2255–2259. [CrossRef] [PubMed]
23. Perera, S.D.; Mariano, R.G.; Vu, K.; Nour, N.; Seitz, O.; Chabal, Y.; Balkus, K.J. Hydrothermal synthesis of graphene-TiO_2 nanotube composites with enhanced photocatalytic activity. *ACS Catal.* **2012**, *2*, 949–956. [CrossRef]
24. Wang, Y.; Guo, C.; Liu, J.; Chen, T.; Yang, H.; Li, C. CeO_2 nanoparticles/graphene nanocomposite-based high performance supercapacitor. *Dalton. Trans.* **2011**, *40*, 6388–6391. [CrossRef] [PubMed]
25. He, Y.; Chen, W.; Li, X.; Zhang, Z.; Fu, J.; Zhao, C.; Xie, E. Freestanding three-dimensional graphene/MnO_2 composite networks as ultralight and flexible supercapacitor electrodes. *ACS Nano* **2013**, *7*, 174–182. [CrossRef] [PubMed]
26. Li, F.; Zhao, J.; Chen, Z. Fe-anchored graphene oxide: A low-cost and easily accessible catalyst for low-temperature CO oxidation. *J. Phys. Chem. C* **2012**, *116*, 2507–2514. [CrossRef]
27. Song, E.; Wen, Z.; Jiang, Q. CO catalytic oxidation on copper-embedded graphene. *J. Phys. Chem. C* **2011**, *115*, 3678–3683. [CrossRef]
28. Li, N.; Wang, Z.; Zhao, K.; Shi, Z.; Xu, S.; Gu, Z. Graphene-CuO Nanocomposite. *J. Nanosci. Nanotechnol.* **2010**, *10*, 6690–6693. [CrossRef] [PubMed]
29. Hsu, Y.; Hsu, T.; Sun, C.; Nien, Y.; Pu, N.; Ger, M. Synthesis of CuO/graphene nanocomposites for nonenzymatic electrochemical glucose biosensor applications. *Electrochim. Acta* **2012**, *82*, 152–157. [CrossRef]
30. Guo, Y.; Guo, S.; Ren, J.; Zhai, Y.; Dong, S.; Wang, E. Cyclodextrin functionalized graphene nanosheets with high supramolecular recognition capability: Synthesis and host-guest inclusion for enhanced electrochemical performance. *ACS Nano* **2010**, *4*, 4001–4010. [CrossRef] [PubMed]
31. Jin, L.; He, M.; Lu, J.; Luo, M.; Fang, P.; Xie, Y. Comparative Study of CuO Species on CuO/Al_2O_3, CuO/CeO_2-Al_2O_3 and CuO/La_2O-Al_2O_3 Catalysts for CO Oxidation. *Chin. J. Chem. Phys.* **2007**, *20*, 582–586. [CrossRef]
32. Morales, J.; Sánchez, L.; Martín, F.; Ramos-Barrado, J.R.; Sánchez, M. Use of low-temperature nanostructured CuO thin films deposited by spray-pyrolysis in lithium cells. *Thin. Solid Films* **2005**, *474*, 133–140. [CrossRef]
33. Gao, L.; Yue, W.; Tao, S.; Fan, L. Novel strategy for preparation of graphene-Pd, Pt composite, and its enhanced electrocatalytic activity for alcohol oxidation. *Langmuir* **2012**, *29*, 957–964. [CrossRef] [PubMed]
34. Hummers, W.S.; Offeman, R.E. Preparation of graphitic oxide. *J. Am. Chem. Soc.* **1958**, *80*, 1339. [CrossRef]